Gravitational wave asteroseismology reexamined

Omar Benhar,[2,1] Valeria Ferrari,[1,2] and Leonardo Gualtieri[1,2]

[1]*Dipartimento di Fisica "G. Marconi", Universitá degli Studi di Roma, "La Sapienza", P.le A. Moro 2, 00185 Roma, Italy*

[2]*INFN, Sezione Roma 1, P.le A. Moro 2, 00185 Roma, Italy*

(Received 26 July 2004; published 10 December 2004)

The frequencies and damping times of the non radial oscillations of non rotating neutron stars are computed for a set of recently proposed equations of state (EOS) which describe matter at supranuclear densities. These EOS are obtained within two different approaches, the nonrelativistic nuclear many-body theory and the relativistic mean field theory, that model hadronic interactions in different ways leading to different composition and dynamics. Being the non radial oscillations associated to the emission of gravitational waves, we fit the eigenfrequencies of the fundamental mode and of the first pressure and gravitational-wave mode (polar and axial) with appropriate functions of the mass and radius of the star, comparing the fits, when available, with those obtained by Andersson and Kokkotas in 1998. We show that the identification in the spectrum of a detected gravitational signal of a sharp pulse corresponding to the excitation of the fundamental mode or of the first p-mode, combined with the knowledge of the mass of the star—the only observable on which we may have reliable information—would allow to gain interesting information on the composition of the inner core. We further discuss the detectability of these signals by gravitational detectors.

DOI: 10.1103/PhysRevD.70.124015 PACS numbers: 04.30.–w, 04.30.Db, 97.60.Jd

I. INTRODUCTION

When a neutron star (NS) is perturbed by some external or internal event, it can be set into non radial oscillations, emitting gravitational waves at the characteristic frequencies of its quasinormal modes. This may happen, for instance, as a consequence of a glitch, of a close interaction with an orbital companion, of a phase transition occurring in the inner core or in the aftermath of a gravitational collapse. The frequencies and the damping times of the quasinormal modes (QNM) carry information on the structure of the star and on the status of nuclear matter in its interior. In 1998, extending a previous work of Lindblom and Detweiler [1], Andersson and Kokkotas computed the frequencies of the fundamental mode (f-mode), of the first pressure mode (p_1-mode) and of the first polar wave mode (w_1-mode) [2] of a non rotating NS for a number of equations of state (EOS) for superdense matter available at that time, the most recent of which was that obtained by Wiringa, Fiks & Fabrocini in 1988 [3]. They fitted the data with appropriate functions of the macroscopical parameters of the star, the radius and the mass, and showed how these empirical relations could be used to put constraints on these parameters if the frequency of one or more modes could be identified in a detected gravitational signal. It should be stressed that, while the mass of a NS can be determined with a good accuracy if the star is in a binary system, the same cannot be said for the radius which, at present, is very difficult to determine through astronomical observations; it is therefore very interesting to ascertain whether gravitational-wave detection would help in putting constraints on this important parameter. Knowing the mass and the radius, we would also gain information on the state and composition of matter at the extreme densities and pressures that prevail in a NS core and that are unreachable in a laboratory.

For instance, it has long been recognized that the Fermi gas model, which leads to a simple polytropic EOS, yields a maximum NS mass $\sim 0.7\ M_\odot$ that dramatically fails to explain the observed NS masses; this failure clearly shows that NS equilibrium requires a pressure other than the degeneracy pressure, the origin of which has to be traced back to the nature of hadronic interactions. Unfortunately, the need of including dynamical effects in the EOS is confronted with the complexity of the fundamental theory of strong interactions, quantum chromo dynamics (QCD). As a consequence, all available models of the EOS of strongly interacting matter have been obtained within models, based on the theoretical knowledge of the underlying dynamics and constrained, as much as possible, by empirical data.

In recent years, a number of new EOS have been proposed to describe matter at supranuclear densities ($\rho > \rho_0,\ \rho_0 = 2.67 \cdot 10^{14}\ \mathrm{g/cm^3}$ being the equilibrium density of nuclear matter), some of them allowing for the formation of a core of strange baryons and/or deconfined quarks, or for the appearance of a Bose condensate. The present work is aimed at verifying whether, in the light of the recent developments, the empirical relations derived in [2] are still appropriate or need to be updated.

We consider a variety of EOS, described in detail in Sec. II. For any of them we obtain the equilibrium, non rotating, configurations for assigned values of the mass, we solve the equations of stellar perturbations and compute the frequencies of the quasinormal modes of vibration. The results obtained for the different EOS are compared, looking for particular signatures in the behav-

ior of the mode frequencies, which we plot as functions of the various physical parameters: mass, compactness (M/R), average density. Finally, we fit the data with suitable functions of M and R and see whether the fits agree with those of Andersson and Kokkotas. We extend the work done in [2], and a similar analysis carried out in [4] for the axial modes, in several respects: we construct models of neutron stars with a composite structure, formed of an outer crust, an inner crust and a core, treating the matter composing the star as a non viscous fluid which obeys equations of state appropriate to describe different density regions (at the interface of layers of different composition we match the EOS, the metric functions and their derivatives continuously). We choose for the inner core recent EOS which model hadronic interactions in different ways leading to different composition and dynamics; we include in our study further classes of modes (the axial w-modes and the axial and polar w_{II}-modes). Results and fits are discussed in Sec. III.

II. OVERVIEW OF NEUTRON STAR STRUCTURE

The internal structure of NS is believed to feature a sequence of layers of different composition. While the properties of matter in the outer crust, corresponding to densities ranging from $\sim 10^7$ g/cm^3 to the neutron drip density $\rho_d = 4 \times 10^{11}$ g/cm^3, can be obtained directly from nuclear data, models of the EOS at $4 \times 10^{11} < \rho < 2 \times 10^{14}$ g/cm^3 are somewhat based on extrapolations of the available empirical information, as the extremely neutron rich nuclei appearing in this density regime are not observed on earth. In the present work we have employed two well established EOS for the outer and inner crust: the Baym-Pethick-Sutherland (BPS) EOS [5] and the Pethick-Ravenhall-Lorenz (PRL) EOS [6], respectively.

The density of the NS core ranges between $\sim \rho_0$, at the boundary with the inner crust, and a central value that can be as large as $1 \div 4 \times 10^{15}$ g/cm^3. All models of EOS based on hadronic degrees of freedom predict that in the density range $\rho_0 \lesssim \rho \lesssim 2\rho_0$ NS matter consists mainly of neutrons, with the admixture of a small number of protons, electrons and muons. At any given density the fraction of protons and leptons is determined by the requirements of weak equilibrium and charge neutrality.

This picture may change significantly at larger density with the appearance of heavy strange baryons produced in weak interaction processes. For example, although the mass of the Σ^- exceeds the neutron mass by more than 250 MeV, the reaction $n + e^- \rightarrow \Sigma^- + \nu_e$ is energetically allowed as soon as the sum of the neutron and electron chemical potentials becomes equal to the Σ^- chemical potential.

Finally, as nucleons are known to be composite objects of size $\sim 0.5 - 1.0$ fm, corresponding to a density $\sim 10^{15}$ g/cm^3, it is expected that if the density in the NS core reaches this value matter undergoes a transition to a new phase, in which quarks are no longer clustered into nucleons or hadrons.

Models of the nuclear matter EOS $\rho \geq \rho_0$ are mainly obtained within two different approaches: nonrelativistic nuclear many-body theory (NMBT) and relativistic mean field theory (RMFT).

In NMBT, nuclear matter is viewed as a collection of pointlike protons and neutrons, whose dynamics is described by the nonrelativistic Hamiltonian:

$$H = \sum_i \frac{p_i^2}{2m} + \sum_{j>i} v_{ij} + \sum_{k>j>i} V_{ijk}, \qquad (1)$$

where m and p_i denote the nucleon mass and momentum, respectively, whereas v_{ij} and V_{ijk} describe two- and three-nucleon interactions. The two-nucleon potential, that reduces to the Yukawa one-pion-exchange potential at large distance, is obtained from an accurate fit to the available data on the two-nucleon system, i.e. deuteron properties and $\sim$4000 nucleon-nucleon scattering phase shifts [7]. The purely phenomenological three-body term V_{ijk} has to be included in order to account for the binding energies of the three-nucleon bound states [8].

The many-body Schrödinger equation associated with the Hamiltonian of Eq. (1) can be solved exactly, using stochastic methods, for nuclei with mass number up to 10. The energies of the ground and low-lying excited states are in excellent agreement with the experimental data [9]. Accurate calculations can also be carried out for uniform nucleon matter, exploiting translational invariace and using either a variational approach based on cluster expansion and chain summation techniques [10], or G-matrix perturbation theory [11].

Within RMFT, based on the formalism of relativistic quantum field theory, nucleons are described as Dirac particles interacting through meson exchange. In the simplest implementation of this approach the dynamics is modeled in terms of a scalar and a vector field [12].

Unfortunately, the equations of motion obtained minimizing the action turn out to be solvable only in the mean field approximation, i.e., replacing the meson fields with their vacuum expectation values, which amounts to treating them as classical fields. Within this scheme the nuclear matter EOS can be obtained in closed form and the parameters of the Lagrangian density, i.e., the meson masses and coupling constants, can be determined by fitting the empirical properties of nuclear matter, i.e., binding energy, equilibrium density and compressibility.

NMBT and RMFT can be both generalized to take into account the appearance of strange baryons. However, very little is known of their interactions. The available models of the hyperon-nucleon potential [13] are only loosely constrained by few data, while no empirical information is available on hyperon-hyperon interactions.

NMBT, while suffering from the limitations inherent in its nonrelativistic nature, is strongly constrained by data and has been shown to possess a highly remarkable predictive power. On the other hand, RMFT is very elegant but assumes a somewhat oversimplified dynamics, which is not constrained by nucleon-nucleon data. In addition, it is plagued by the uncertainty associated with the use of the mean field approximation, which is long known to fail in strongly correlated systems (see, e.g., Ref. [14]).

In our study we shall also consider the possibility that a transition to quark matter may occur at sufficiently high density. Because of the complexity of QCD, a first principle description of the EOS of quark matter at high density and low temperature is out of reach of present theoretical calculations. A widely used alternative approach is based on the MIT bag model [15], the main assumptions of which are that (i) quarks are confined to a region of space (the bag) whose volume is limited by the pressure B (the bag constant), and (ii) interactions between quarks are weak and can be neglected or treated in lowest order perturbation theory.

Below, we list the different models of EOS employed in our work to describe NS matter at $\rho > 2 \times 10^{14}$ g/cm^3, i.e., in the star core. As already stated, all models have been supplemented with the PRL and BPS EOS for the inner and outer crust, respectively.

(i) APR2. Matter consists of neutrons, protons, electrons and muons in weak equilibrium. The EOS is obtained within NMBT using the Argonne v_{18} two-nucleon potential [7] and the Urbana IX three-nucleon potential [8]. The many-body Schrödinger equation is solved within a variational approach [10,16]. The calculation includes relativistic corrections to the two-nucleon potential, arising from the boost to a frame in which the total momentum of the interacting pair is nonvanishing. These corrections are necessary to use phenomenological potentials, describing interactions between nucleons in their center of mass frame, in a locally inertial frame associated with the star. The maximun mass for this EOS is $M_{\rm max} = 2.202\ M_\odot$.

(ii) APRB200, APRB120. These models are obtained combining a lower density phase, extending up to $\sim 4\rho_0$ and described by the APR2 nuclear matter EOS, with a higher density phase of deconfined quark matter described within the MIT bag model. Quark matter consists of massless up and down quarks and massive strange quarks, with $m_s = 150$ MeV, in weak equilibrium. One-gluon-exchange interactions between quarks of the same flavor are taken into account at first order in the color coupling constant, set to $\alpha_s = 0.5$. The value of the bag constant is 200 and 120 MeV/fm^3 in the APR200 and APR120 model, respectively. The phase transition is described requiring the fulfillment of Gibbs conditions, leading to the formation of a mixed phase, and neglecting surface and Coulomb effects [10,17]. The maximum mass is $M_{\rm max} = 2.029\ M_\odot$ for APRB200 and $M_{\rm max} = 1.894\ M_\odot$ for APRB120.

(iii) BBS1. Matter composition is the same as in the APR2 model. The EOS is obtained within NMBT using a slightly different Hamiltonian, including the Argonne v_{18} two-nucleon potential and the Urbana VII three-nucleon potential [18]. The ground state energy is calculated using G-matrix perturbation theory [19]. The maximum mass is $M_{\rm max} = 2.014\ M_\odot$.

(iv) BBS2. Matter consists of nucleons leptons and strange heavy baryons (Σ^- and Λ^0). Nucleon interactions are described as in BBS1. Hyperon-nucleon interactions are described using the potential of Ref. [13], while hyperon-hyperon interactions are neglected altogether. The binding energy is obtained from G-matrix perturbation theory [19]. The maximum mass is $M_{\rm max} = 1.218 M_\odot$.

(v) G240. Matter composition includes leptons and the complete octet of baryons (nucleons, $\Sigma^{0,\pm}$, Λ^0 and $\Xi^\pm$). Hadron dynamics is described in terms of exchange of one scalar and two vector mesons. The EOS is obtained within the mean field approximation [20]. The maximum mass is $M_{\rm max} = 1.553\ M_\odot$.

In addition to the above models we have considered the possibility that a star entirely made of quarks (strange star) may form. The existence of strange stars is predicted as a consequence of the hypotesis, suggested by Bodmer [21] and Witten [22], that the ground state of strongly interacting matter consist of up, down and strange quarks. In the limit in which the mass of the strange quark can be neglected, the density of quarks of the three flavors is the same and charge neutrality is guaranteed even in absence of leptons. To gauge the difference between this exotic scenario and the more conventional ones, based mostly on hadronic degrees of freedom, we have calculated the EOS of strange quark matter within the MIT bag model, setting all quark masses and the color coupling constant to zero and choosing $B = 110$ MeV/fm^3. The models denoted SS1 and SS2 correspond to a quark star with a crust, described by the BPS EOS and extending up to neutron drip density, and to a bare quark star, respectively.

For any of the above EOS the equilibrium NS configurations have been obtained solving the Tolman Oppenheimer Volkoff (TOV) equations for different values of the central density. However, comparison of the calculated maximum masses with the NS masses obtained from observations, ranging between ~ 1.1 and

$\sim 1.9\ M_\odot$ [23,24], does not provide a stringent test on the EOS, as most models support a stable star configuration with mass compatible with the data. Valuable additional information may come from recent studies aimed at determining the NS mass-radius ratio. Cottam *et al.* [25] have reported that the Iron and Oxygen transitions observed in the spectra of 28 bursts of the X-ray binary EXO0748-676 correspond to a gravitational redshift $z = 0.35$, yielding in turn a mass-radius ratio $M/R = 0.153\ M_\odot/\mathrm{km}$.

Figure 1 shows the dependence of the neutron star mass upon its radius for the model EOS employed in this work. Although the results of Ref. [25] are still somewhat controversial, it appears that the EOS based on nucleonic degrees of freedom (APR2, BBS1), strongly constrained by nuclear data and nucleon-nucleon scattering, fulfill the requirement of crossing the redshift line within the band corresponding to the observationally allowed masses. While the possible addition of quark matter in a small region in the center of the star (APRB200, APRB120) does not dramatically change the picture, the occurrence of a transition to hyperonic matter at densities as low as twice the equilibrium density of nuclear matter leads to a sizable softening of the EOS (BBS2 , G240), thus making the mass-radius relation incompatible with that resulting from the redshift measurement of Cottam *et al.* [25]. The models of strange star we have considered (SS1, SS2) also appear to be compatible with observations, irrespective of the presence of a crust, but the corresponding radius turns out to be significantly smaller than the ones predicted by any other EOS. It has to be kept in mind, however, that strange star models imply a high degree of arbitrariness in the choice of the bag model parameters,

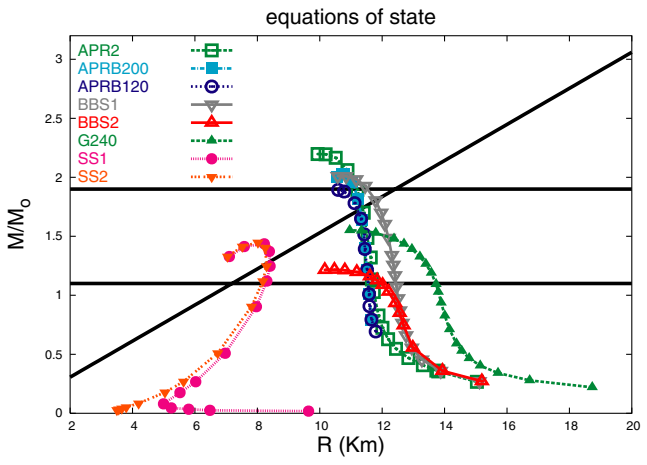

FIG. 1 (color online). NS mass versus radius for the models of EOS described in the text. The two horizontal lines denote the boundaries of the region of observationally allowed NS masses, while the straight crossing line corresponds to the mass-radius relation extracted from the redshift measurement of Cottam *et al.* (2002)

that may lead to results appreciably different from one another. For example, the mass-radius relations obtained from the models of Dey *et al.* [26] turn out to be inconsistent with a redshift $z = 0.35$ [25].

III. THE QUASI-NORMAL MODE FREQUENCIES

To find the frequencies and damping times of the quasinormal modes we solve the equations describing the non radial perturbations of a non rotating star in general relativity. These equations are derived by expanding the perturbed tensors in tensorial spherical harmonics in an appropriate gauge, closing the system with the selected EOS. The perturbed equations split into two distinct sets, the *axial* and the *polar* which belong, respectively, to the harmonics that transform like $(-1)^{(\ell+1)}$ and $(-1)^\ell$ under the parity transformation $\theta \to \pi - \theta$ and $\varphi \to \pi + \varphi$. A quasinormal mode of the star is defined to be a solution of the perturbed equations belonging to complex eigenfrequency, which is regular at the center and continuous at the surface, and which behaves as a pure outgoing wave at infinity. The real part of the frequency is the pulsation frequency, the imaginary part is the inverse of the damping time of the mode due to gravitational-wave emission. It is customary to classify the QNM according to the source of the restoring force which prevails in bringing the perturbed element of fluid back to the equilibrium position. Thus, we have a g-mode if the restoring force is mainly provided by buoyancy or a p-mode if it is due to a gradient of pressure. The frequencies of the g-modes are lower than those of the p-modes, the two sets being separated by the frequency of the fundamental mode, which is related to the global oscillations of the fluid. In general relativity there exist further modes that are purely gravitational since they do not induce fluid motion, named w-modes [27,28]. The w-modes are both polar and axial, they are highly damped and, in general, their frequencies are higher than the p-mode frequencies, apart from a branch, named w_{II}, for which the frequencies are comparable to those of the p-modes.

We integrate the perturbed equations in the frequency domain. For the polar ones, we integrate the set of equations used in [29]; for each assigned value of the harmonic index l and of the frequency ν, they admit only two linearly independent solutions regular at $r = 0$. The general solution is found as a linear combination of the two, such that the Lagrangian perturbation of the pressure vanishes at the surface. Outside the star, the solution is continued by integrating the Zerilli equation to which the polar equations reduce when the fluid perturbations vanish [30]. For the axial perturbations we integrate the Schrödingerlike equation derived in [31].

To explicitely compute the QNM eigenfrequencies we follow two different procedures: for the slowly damped modes, i.e., those, as the f- and p-modes, for

which the imaginary part of the frequency is much smaller than the real part we use the algorithm developed in [31,32]: the perturbed equations are integrated for real values of the frequency from $r = 0$ to radial infinity, where the amplitude of the Zerilli function is computed; the frequency of a QNM can be shown to correspond to a local minimum of this function and the damping time is given in terms of the width of the parabola which fits the wave amplitude as a function of the frequency near the minimum. We shall indicate this method as the CF-algorithm.

For highly damped modes, when the imaginary part of the frequency is comparable to (or greather than) the real part, the CF-algorithm cannot be applied and we use the continued fractions method [33], integrating the perturbed equations in the complex frequency domain. With this method we find the frequencies of the axial and polar w-modes. A clear account on continued fractions can be found in [34]. However, it should be mentioned that this algorithm cannot be applied when $M/R \geq 0.25$, and therefore the w-mode frequencies cannot be computed for ultracompact stars.

The parameters of the stellar models coneesidered in this study are shown in the Appendix.

A. Fits and Plots

As done in Ref. [2], the frequencies and damping times of the various modes can be fitted by suitable functions of the mass and of the radius of the NS. In computing the fit parameters, we shall exclude the data referring to strange stars, because there is a very large degree of arbitrariness in the choice of the bag model parameters; conversely, the EOS from which we derive the empirical relations fit at least some (or many) experimental data on nuclear properties and nucleon-nucleon scattering and/or some observational data on NSs. However, in all figures we shall also plot the data corresponding to strange stars for comparison.

In Refs. [2,35] it was shown how the fits should be used to set stringent constraints on the mass and radius of the star provided the frequency and the damping times of some of the modes are detected in a gravitational signal, and we shall not repeat the analysis here. We shall rather focus on a different aspect of the problem showing that, if we know the mass of the star, the QNM frequencies can be used to gain direct information on the EOS of nuclear matter, and to this purpose we shall plot the mode frequencies as a function of the stellar mass.

Let us consider the fundamental mode firstly. Numerical simulations show that this is the mode which is mostly excited in many astrophysical processes and consequently the major contribution to gravitational-wave emission should be expected at this frequency. Moreover, as for the p-modes, its damping time is quite long compared to that of the w-modes, therefore it should appear in the spectrum of the gravitational signal as a sharp peak and should be easily identifiable.

It is known from the Newtonian theory of stellar perturbations that the f-mode frequency scales as the square root of the average density; indeed, our numerical results for the f-mode can be fitted by the following expression

$$\nu_f = a + b\sqrt{\frac{M}{R^3}}, \quad a = 0.79 \pm 0.09, \quad b = 33 \pm 2, \quad (2)$$

where a is given in kHz and b in km $\times$ kHz. In this fit and hereafter in all fits, frequencies will be expressed in kHz, masses and radii in km, damping times in s and $c = 3 \times 10^5$ km/s.

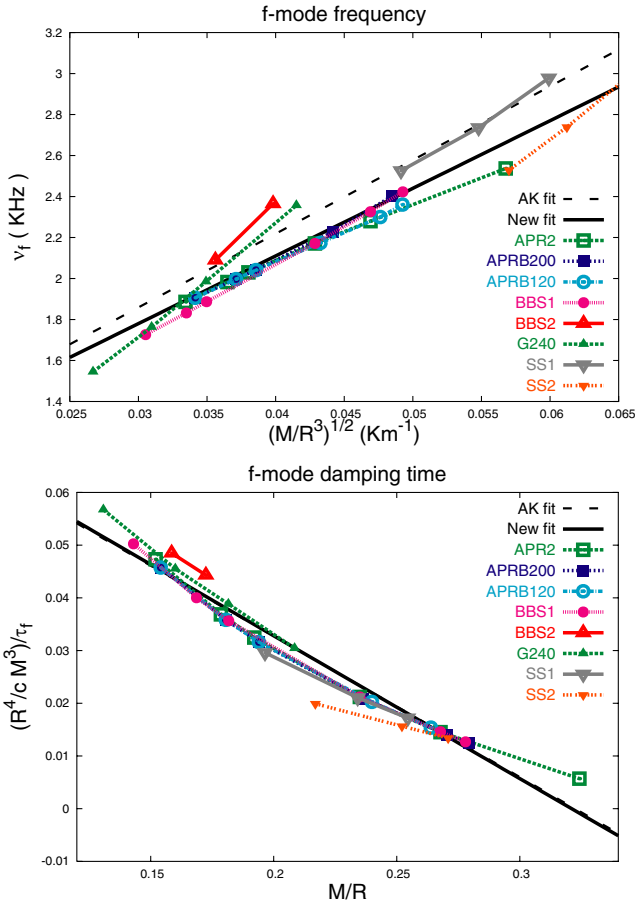

FIG. 2 (color online). The frequency of the fundamental mode is plotted in the upper panel as a function of the square root of the average density for the different EOS considered in this paper. We also plot the fit given by Andersson and Kokkotas (AK-fit) and our fit (New fit). The new fit is systematically lower (about 100 Hz) than the old one. The damping time of the fundamental mode is plotted in the lower panel as a function of the compactness M/R. The AK-fit and our fit, plotted, respectively, as a dashed and continuous line, do not show significant differences.

In a similar way, the damping time of the f-mode can be fitted as a function of the compactness M/R as follows

$$\tau_f = \frac{R^4}{cM^3}\left[a + b\frac{M}{R}\right]^{-1},$$
$$a = [8.7 \pm 0.2] \times 10^{-2}, \qquad b = -0.271 \pm 0.009. \tag{3}$$

The data for the f-mode and the fits are shown in Fig. 2. In the upper panel we plot ν_f versus M/R^3, for all considered stellar models. The fit (2) is plotted as a thick solid line, and the fit given in [2], which is based on the EOSs considered in that paper, is plotted as a dashed line labeled as "AK-fit". In the lower panel we plot the damping time τ_f versus the compactness M/R, our fit and the corresponding AK-fit.

From Fig. 2 we see that our new fit for ν_f is systematically lower than the AK-fit by about 100 Hz; this basically shows that the new EOS are, on average, less compressible (i.e., stiffer) than the old ones. Conversely, Eq. (3) is very similar to the fit found in [2].

The frequency of the first p-mode, and of the first polar and axial w- and w^{II}-modes can be fitted as a function of the compactness as follows

$$\nu = \frac{1}{K}\left[a + b\frac{M}{R}\right], \tag{4}$$

where $K = M$ for ν_{p_1}, $\nu^{\rm pol}_{w^{II}_1}$ and $\nu^{\rm ax}_{w^{II}_1}$, whereas $K = R$ for $\nu^{\rm pol}_{w_1}$ and $\nu^{\rm ax}_{w_1}$. The parameters of the fit, a and b, are given in Table I.

The data and the fit for the mode p_1 are shown in Fig. 3. In the upper panel we plot ν_{p_1} multiplied by the stellar mass M, the new fit and the corresponding AK-fit, versus the star compactness; it can be noted that the two fits have a different slope. In the lower panel the inverse of the damping time multiplied by the mass (M/τ_p) is plotted versus M/R: the spread of the data is apparent. Indeed, as already noted in [2], in this case a fit has no significance.

For the remaining axial and polar w-modes we find that the damping times are very well fitted by suitable functions of the compactness as follows

$$\tau = 10^{-3} \times M\left[c + d\frac{M}{R} + e\left(\frac{M}{R}\right)^2\right]^{-1}, \tag{5}$$

where c, d and e, expressed in km/s, are given in Table I.

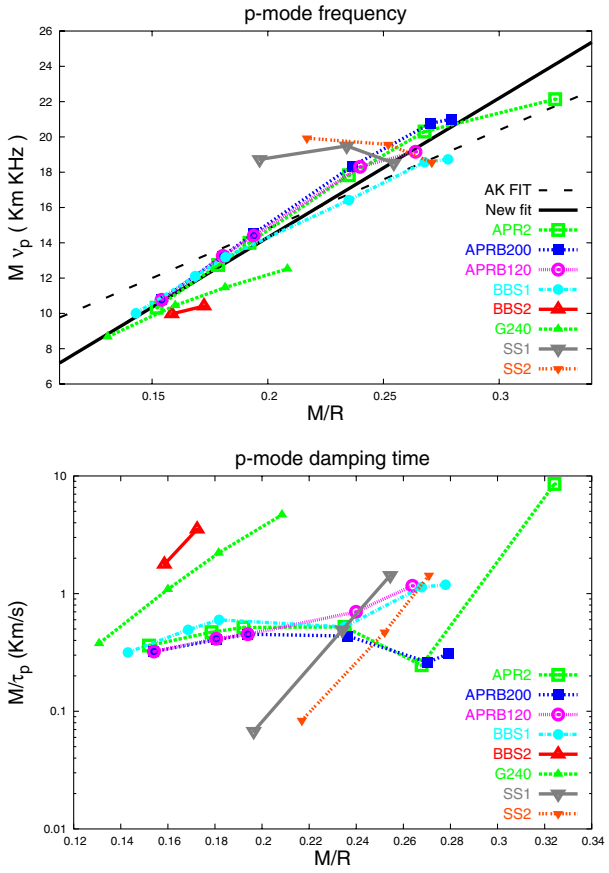

FIG. 3 (color online). The frequency (upper panel) and the damping time (lower panel) of the first p-mode are plotted as a function of the compactness of the star. The AK-fit and the new fit for the frequency are plotted, in the upper panel, as a dashed and continuous line, respectively. As already noted in [2] the data referring to the damping time are so spread that a fit has no significance.

We do not plot all fits and data for the w-modes because the graphs would not add more relevant information.

The empirical relations derived above could be used, as described in [2,35], to determine the mass and the radius of the star from the knowledge of the frequency and damping time of the modes; but now we want to address a different question: we want to understand whether the knowledge of the mode frequencies and of the mass of the star, which is after all the only observable on which we

TABLE I. The values of the parameters of the fits given by Eqs. (4) and (5) are given for the first p-mode and for the first axial and polar w modes (see text)

Mode	a	b	c	d	e
p_1	-1.5 ± 0.8	79 ± 4	...	...	...
w_1^{pol}	215 ± 1.3	-474 ± 7	36 ± 19	720 ± 200	-2300 ± 500
w_1^{IIpol}	-5.8 ± 0.4	102 ± 2	21 ± 16	700 ± 170	-1400 ± 500
w_1^{ax}	121 ± 2	-146 ± 12	48 ± 6	360 ± 70	-1340 ± 170
w_1^{IIax}	-13.1 ± 0.4	110 ± 2	-7 ± 11	1400 ± 120	-2700 ± 300

might have reliable information, can help in discriminating among the different EOSs. To this purpose in Fig. 4 and 5 we plot, respectively, ν_f and ν_p as a function of the mass, for all EOS and all stellar models.

We notice that the presence of quark matter in the star inner core (EOS APRB200 and APRB120) does not seem to significantly affect the pulsation properties of the star. This is a generic feature, which we observe also in the p- and w- modes behavior.

From Fig. 4 we also see that the BBS1 and APR2 EOS, based un similar dynamical models, yield appreciably different f-mode frequencies. This is likely to be ascribed to the effect of the relativistic corrections included in the APR2 EOS and to different treatments of three-nucleon interactions. While the variational approach of Ref. [10], used to derive the APR2 EOS naturally allows for inclusion of the three-nucleon potential appearing in Eq. (1), in G-matrix perturbation theory, used to derive the BBS1 EOS, V_{ijk} has to be replaced with an effective two-nucleon potential $\tilde{V}_{ij}$, obtained by averaging over the position of the third particle [36].

The transition to hyperonic matter, predicted by the BBS2 model, produces a sizable softening of the EOS, thus leading to stable NS configurations of very low mass. As a consequence of the softening of the EOS, the corresponding f-mode frequency is significantly higher than those obtained with the other EOS. So much higher, in fact, that its detection would provide evidence of the presence of hyperons in the NS core.

It is also interesting to compare the f-mode frequencies corresponding to models BBS2 and G240 , as they both predict the occurrence of heavy strange baryons but are obtained from different theoretical approaches, based on different descriptions of the underlying dynamics. The behavior of ν_f displayed in Fig. 4 directly reflects the relations between mass and central density obtained from the two EOS, larger frequencies being always associated with larger densities. For example, the NS configurations of mass $\sim 1.2\ M_\odot$ obtained from the G240 and BBS2 have central densities $\sim 7 \times 10^{14}$ g/cm^3 and $\sim 2.5 \times 10^{15}$ g/cm^3, respectively. On the other hand, the G240 model requires a central density of $\sim 2.5 \times 10^{15}$ g/cm^3 to reach a mass of $\sim 1.55\ M_\odot$ and a consequent ν_f equal to that of the BBS2 model.

Strange stars models, SS1 and SS2 also correspond to values of ν_f and ν_p well above those obtained from the other models. The peculiar properties of these stars, which are also apparent from the mass-radius relation shown in Fig. 1 largely depend upon the self-bound nature of strange quark matter.

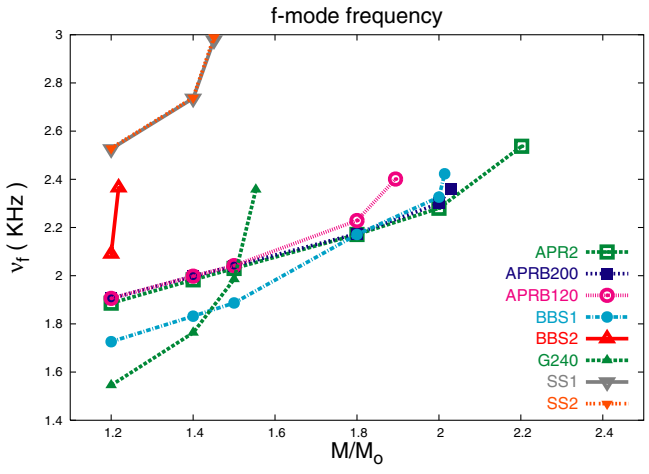

FIG. 4 (color online). The frequency of the fundamental mode is plotted as a function of the mass of the star.

IV. CONCLUDING REMARKS

Having shown how the internal structure affects the frequencies at which a neutron star oscillates and emits gravitational waves, it is interesting to ask whether the present generation of gravitational antennas may actually detect these signals. To this purpose, let us consider, as an example, a neutron star with an inner core composed of nuclear matter satisfying the EOS APR2 . Be $M = 1.4 M_\odot$ its mass, and let us assume that its fundamental mode ($\nu_f = 1983 Hz$, $\tau_f = 0.184 s$) has been excited by some external or internal event. The signal emitted by the star can be modeled as a damped sinusoid [37]

$$h(t) = \mathcal{A} e^{(t_{\rm arr}-t)/\tau_f} \sin[2\pi\nu_f(t - t_{\rm arr})], \tag{6}$$

where $t_{\rm arr}$ is the arrival time and $\mathcal{A}$ is the mode amplitude; the energy stored into the mode can be estimated by integrating over the surface and over the frequency the expression of the energy flux

$$\frac{dE_{\rm mode}}{dSd\nu} = \frac{\pi}{2}\nu^2|\tilde{h}(\nu)|^2, \tag{7}$$

where $h(\nu)$ is the Fourier-transorm of $h(t)$. Would we be able to detect this signal with, say, the ground based interferometric antenna VIRGO?

The VIRGO noise power spectral density can be modeled as [38]

$$S_n(x) = 10^{-46} \times \{3.24[(6.23x)^{-5} + 2x^{-1} + 1 + x^2]\} Hz^{-1}, \tag{8}$$

where $x = \nu/\nu_0$, with $\nu_0 = 500$ Hz; at frequencies lower than the cutoff frequency $\nu_s = 20$ Hz the noise sharply increases. Assuming that we extract the signal from noise by using the optimal matched filtering technique, the signal to noise ratio (SNR) can easily be computed from the following expression

$$SNR = 2\left[\int_0^\infty d\nu \frac{|\tilde{h}(\nu)|^2}{S_n(\nu)}\right]^{1/2}. \tag{9}$$

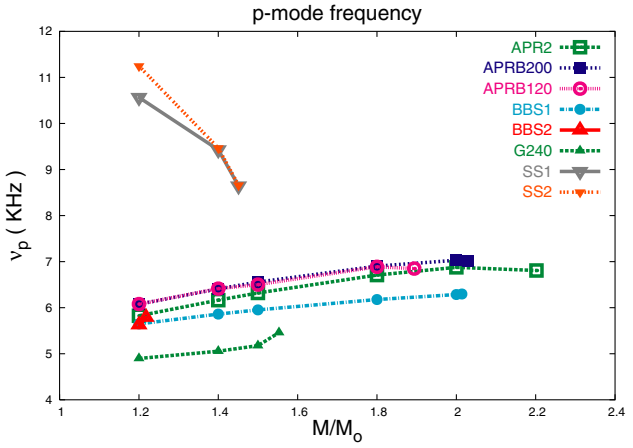

FIG. 5 (color online). The frequency of the first p-mode is plotted as a function of the mass of the star.

Using Eqs. (6)–(9) we find that in order to reach, say, SNR $= 5$, the energy stored into the f-mode should be $E_{f\text{-mode}} \sim 6 \times 10^{-7}\, M_\odot c^2$ for a source in our Galaxy (distance from Earth $d \sim 10$ kpc) and $E_{f\text{-mode}} \sim 1.3\, M_\odot c^2$ for a source in the VIRGO cluster ($d \sim 15$ Mpc). Similar estimates can be found for the detectors LIGO, GEO, TAMA.

These numbers indicate that it is unlikely that the first generation of interferometric antennas will detect the gravitational waves emitted by an oscillating neutron star. However, new detectors are under investigation that should be much more sensitive at frequencies above 1–2 kHz and that would be more appropriate to detect these signals.

If the frequencies of the modes will be identified in a detected signal, the simultaneous knowledge of the mass of the emitting star will be crucial to understand its internal composition. Indeed, as shown in Figs. 4 and 5, we would be able for instance to infer, or exclude, the presence of strange baryons in the inner core, and to see whether nature allows for the formation of bare strange stars. We remark that, in particular, the f-mode and the first p-modes, that numerical simulations indicate as those that are most likely to be excited [39,40], have relatively long damping times, and therefore their excitation should appear in the spectrum as a sharp peak at the corresponding frequency, a feature that would facilitate their identification.

TABLE II. Parameters of the considered stellar models: for each EOS and for each assigned value of the stellar mass, we give the central density ρ_c in units of $\rho_0 = 10^{15}$ g/cm^3, the radius R in km and the compactness M/R (M and R in km). Empty slots refer to masses that exceed the maximum mass.

		$1.2M_\odot$	$1.4M_\odot$	$1.5M_\odot$	$1.8M_\odot$	$2M_\odot$	$M_{\max}$
APR2	ρ_c/ρ_0	0.884	0.994	1.056	1.294	1.562	2.749
	R (km)	11.66	11.58	11.53	11.31	11.03	10.03
	M/R	0.152	0.179	0.192	0.235	0.268	0.325
APRB200	ρ_c/ρ_0	0.890	0.996	1.056	1.285	1.795	2.457
	R (km)	11.50	11.45	11.42	11.24	10.92	10.73
	M/R	0.154	0.181	0.194	0.236	0.270	0.279
APRB120	ρ_c/ρ_0	0.890	0.997	1.080	1.540	···	2.516
	R (km)	11.50	11.45	11.42	11.08	···	10.60
	M/R	0.154	0.181	0.194	0.240	···	0.264
BBS1	ρ_c/ρ_0	0.766	0.888	0.960	1.289	2.061	2.509
	R (km)	12.39	12.26	12.19	11.80	11.03	10.70
	M/R	0.143	0.169	0.182	0.225	0.268	0.279
BBS2	ρ_c/ρ_0	1.811	···	···	···	···	2.666
	R (km)	11.18	···	···	···	···	10.43
	M/R	0.159	···	···	···	···	0.172
G240	ρ_c/ρ_0	0.712	1.070	1.525	···	···	2.565
	R (km)	13.55	12.92	12.20	···	···	11.00
	M/R	0.131	0.160	0.182	···	···	0.208
SS1	ρ_c/ρ_0	1.638	2.448	···	···	···	3.771
	R (km)	9.02	8.83	···	···	···	8.42
	M/R	0.197	0.234	···	···	···	0.255
SS2	ρ_c/ρ_0	1.641	2.453	···	···	···	3.777
	R (km)	8.17	8.20	···	···	···	7.91
	M/R	0.217	0.252	···	···	···	0.271

ACKNOWLEDGMENTS

The authors are grateful to M. Baldo, F. Burgio, V. R. Pandharipande and D. G. Ravenhall for providing tables of their EOS.

APPENDIX

In Table II we tabulate the parameters of the equilibrium configurations of the non rotating stars we consider in this paper: the central density in g/cm^3, the stellar radius in km and the compactness M/R (M and R in km), for assigned values of the gravitational mass, that range from 1.2 $M_\odot$ to the maximum mass.

The frequencies and damping times of the quasinormal modes, obtained by integrating the equations of stellar perturbations for these stellar models and for $l = 2$, are available online at http://chimera.roma1.infn.it/OMAR/GW.

[1] L. Lindblom, S. Detweiler, Astrophys. J. Suppl. Ser. **53**, 73 (1983).

[2] N. Andersson, K. D. Kokkotas, Mon. Not. R. Astron. Soc. **299**, 1059, (1998).

[3] R. B. Wiringa, V. Fiks, and A. Fabrocini, Phys. Rev. C **38**, 1010, (1988).
[4] O. Benhar, E. Berti, and V. Ferrari, Mon. Not. R. Astron. Soc. **310**, 797 (1999).
[5] G. Baym, C. J. Pethick, and P. Sutherland, Astrophys. J. **170**, 299 (1971).
[6] C. J. Pethick, B. G. Ravenhall, and C. P. Lorenz, Nucl. Phys. A **584**, 675 (1995).
[7] R. B. Wiringa, V. G. J. Stoks, and R. Schiavilla, Phys. Rev. C **51**, 38 (1995).
[8] B. S. Pudliner, V. R. Pandharipande, J. Carlson, S. C. Pieper, and R. B. Wiringa, Phys. Rev. C **56**, 1720 (1995).
[9] S. C. Pieper and R. B. Wiringa, Annu. Rev. Nucl. Part. Sci. **51**, 53 (2001).
[10] A. Akmal and V. R. Pandharipande, Phys. Rev. C **56**, 2261 (1997).
[11] M. Baldo, G. Giansiracusa, U. Lombardo, H. Q. Song, Phys. Lett. B **473**, 1 (2000).
[12] J. D. Walecka, Ann. Phys. (N.Y.) **83**, 491 (1974).
[13] P. M. M. Maessen, T. A. Rijken, J. J. deSwart, Phys. Rev. C **40**, 2226 (1989).
[14] L. P. Kadanoff and G. Baym, *Quantum Statistical Mechanics* (Benjamin, New York, 1972).
[15] A. Chodos, R. L. Jaffe, K. Johnson, C. B. Tohm, and V. F. Weisskopf, Phys. Rev. D, **9**, 3471 (1974).
[16] A. Akmal, V R. Pandharipande, and D. G. Ravenhall Phys. Rev. C **58**, 1804 (1998).
[17] R. Rubino, thesis, Università ''La Sapienza'', Roma, (unpublished); O. Benhar and Rubino, astro-ph/0410376.
[18] R. Schiavilla, V. R. Pandharipande, and R. B. Wiringa, Nucl. Phys. A **449**, 219 (1986).
[19] M. Baldo, G. F. Burgio, and H. J. Schulze, Phys. Rev. C, **61**, 055801 (2000).
[20] N. K. Glendenning, *Compact Stars* (Springer, New York, 2000).
[21] A. R. Bodmer, Phys. Rev. D, **4**, 1601, (1971).
[22] E. Witten, Phys. Rev. D **30**, 272 (1984).
[23] S. E. Thorsett and D. Chakrabarty, Astrophys. J., **512**, 288 (1999).
[24] H. Quaintrell, *et al.*, Astron. Astrophys., **401**, 313 (2003).
[25] J. Cottam *et al.*, Nature (London), **420**, 51 (2002).
[26] M. Dey, I. Bombaci, J. Dey, R. Subharthi, and B. C. Samanta, Phys. Lett. B **438**, 123 (1999).
[27] S. Chandrasekhar and V. Ferrari, Proc. R. Soc. London A **434**, 449 (1991).
[28] K. D. Kokkotas and B. F. Schutz, Mon. Not. R. Astron. Soc., **255**, 119 (1992).
[29] G. Miniutti, J. A. Pons, E. Berti, L. Gualtieri, and V. Ferrari, Mon. Not. R. Astron. Soc., **338**, 389 (2003).
[30] J. F. Zerilli, Phys. Rev. D **2**, 2141 (1970).
[31] S. Chandrasekhar and V. Ferrari, Proc. R. Soc. London A **432**, 247 (1991).
[32] S. Chandrasekhar, V. Ferrari, and R. Winston, Proc. R. Soc. London A **434**, 635 (1991).
[33] M. Leins, H. P. Nollert, and M. H. Soffel, Phys. Rev. D **48**, 3467 (1993).
[34] H. Sotani, K. Tominaga, and K. I. Maeda, Phys. Rev. D **65**, 024010 (2001).
[35] N. Andersson and K. D. Kokkotas, Mon. Not. R. Astron. Soc. **320**, 307 (1999).
[36] A. Lejeune, P. Grangé, P. Martzoff, and J. Cugnon, Nucl. Phys. A **453**, 189 (1986).
[37] V. Ferrari, G. Miniutti, and J. A. Pons, Classical Quantum Gravity, **20**, S841 (2003).
[38] T. Damour, B. R. Iyer, and B. S. Sathyaprakash, Phys. Rev. D **57**, 885 (1998).
[39] G. Allen, N. Andersson, K. D. Kokkotas, and B. F. Schutz, Phys. Rev. D **58**, 124012 (1998).
[40] J. A. Pons, E. Berti, L. Gualtieri, G. Miniutti, and V. Ferrari, Phys. Rev. D **65**, 104021 (2002).